

ICGSEE-2013[14th – 16th March 2013]
International Conference on Global Scenario in Environment and Energy

A Soft Switching Boost Converter With Simulation Of Maximum Power Point Tracking For Solar Home Lighting System

Ashutosh Werulkar^{1*}, D. Shankar², P.S.Kulkarni³

¹Department of Electronics and Telecommunication Engineering, St.Vincent Pallotti College of Engineering and Technology, Gavsi Manapur, Wardha Road, Nagpur,MH, 440027,India.

^{2&3}Department of Electrical Engineering, Visvesvaraya National Institute of Technology, Nagpur,MH,India.

**Corres.author: ashutoshwerulkar@gmail.com*

Abstract: The aim of the paper is to design a soft Switching Boost Converter with simulation of Maximum Power point tracking for Solar Home Lighting System. A 37Wp Solar Panel is used for designing the boost Converter using soft switching technique. Microcontroller Atmega32 is used to generate the necessary PWM switching signal for the MOSFETs. Soft-switching boost converter is designed to improve the efficiency of the converter and it is observed that efficiency is increased for wide load variation. WIN AVR Software is used as assembler to generate the required hex file for burning in the microcontroller IC. The designed boost converter is further simulated for Maximum Power Point with constant voltage method using Multisim 10 software and results are obtained for the increased current at various Maximum Power Point voltages.

Keywords: Auxiliary resonant circuit; Microcontroller; Photovoltaic (PV); Soft-switching boost converter; Zero-voltage switching (ZVS).

Nomenclature

I	Output current	Q	Carrier charge ($1.6 \times 10^{-19} \text{ C}$)
V	Output voltage	R_s	Series resistance
R_{sh}	Parallel resistance	I_{sh}	Short circuit current
I_0	Reverse saturation current of the equivalent Diode	T_k	Absolute temperature
n	Dielectric constant	K	Boltzman's constant ($1.38 \times 10^{-23} \text{ W sec}^0 .k^{-1}$).

G_{ST}	Standard insolation	T_{ST}	Standard temperature
G	Environmental insolation	T	Environmental temperature
Γ_{SC-T}	Short circuit current temperature coefficient	S_{SC-T}	Open circuit voltage temperature
a, b	Constants (depends on location)	i_{S1}	Main switch current.
i_{S2}	Auxiliary switch current.	i_L	Main inductor current.
i_{LR}	Resonant inductor current.	I_{min}	Minimum current of the main
I_{max}	Maximum current of the main inductor.	I_{LRmax}	Maximum current of the resonant
Δi_L	Current ripple of the main inductor.	$V_{s,min}$	Minimum output voltage of the solar
$V_{s,max}$	Maximum output voltage of the solar cell.	V_L	Main inductor voltage.
V_{Lr}	Resonant inductor voltage.	V_{cr}	Resonant capacitor voltage.
V_{FW}	Freewheeling voltage drop at mode 4.	$Deff$	Effective duty ratio.

I. Introduction:

As the conventional sources of energy at global level are dwindling fast with corresponding rise in cost, solar photovoltaic energy offers promising alternative source. PV energy is free, limitless, pollution free and distributed throughout the earth. Its only demerit is high initial installation cost. According to the announcement of the National Action Plan on climate change in June 2008, the Government of India has approved Jawaharlal Nehru National Mission (JNNSM) which aims at development and deployment of solar energy technologies in the country to achieve parity with grid power tariff by 2022. The objective of the national solar mission is to establish India as a global leader in solar energy, by creating the policy conditions for its diffusion across the country as quickly as possible. The Solar Cell has nonlinear I-V and P-V characteristics which depend on the irradiation, operating temperature and load condition of the cell. Therefore, DC to DC converters play an important role in the PV systems where they find application as charge controllers, maximum power point trackers and for interfacing the PV source with various categories of loads. The Techno Economic Optimum Sizing of a standalone Solar Photovoltaic System is suggested in¹. A simple fast and reliable technique for charging batteries by solar arrays is proposed in². Design of new solar battery charger technology is proposed in³. A case study of solar PV system is presented for Saga deep Iceland in⁴. Different DC-DC topologies are compared for dynamic climatic conditions of PV systems in Egypt⁵. Soft switching boost converter is explained using microcontroller⁶. A resistive control battery charging is explained in⁷. A dynamic DC to DC buck boost topology is explained for battery charging application in⁸. PV/Battery hybrid power management is explained in⁹. MPP tracking system using matching impedance is explained in¹⁰. Microcontroller based boost converter is explained in¹¹. The analysis of microcontroller based solar charge controller for solar home lighting system is covered in¹². A ZCS solar charge controller using microcontroller is covered in¹³.

This paper proposes a soft switching boost converter for Solar Home Lighting System. The 37Wp Solar Panel's voltage is around 15-17.5 V. It is boosted to 24V using soft switching boost converter with microcontroller. The necessary PWM signal required for Boost converter is generated from Atmega32 Microcontroller. The output of Boost Converter is tested using DC loads of 10W and 20W. The Maximum efficiency of the boost converter is obtained to around 88 %. The same boost converter is further simulated to obtain maximum power through 37Wp solar panel using Multisim software and various MPP readings are obtained. This paper is organized as follows. Characteristics of Solar Cell and module are briefly explained in Section II. The proposed System Design is

explained in Section III. Section IV shows simulation analysis of MPP technique in boost converter using constant voltage method.

II. Characteristics of Solar Cell and Module

Fig.1 shows the equivalent Circuit of a Solar Cell. Equations (1) - (3) describe the behavior of a Solar Cell in mathematical form.

$$I = I_{SC} - I_0 \left\{ \exp \left[\frac{q(V + R_s I)}{nKT_K} \right] - 1 \right\} - \frac{V + R_s I}{R_{th}} \quad (1)$$

$$\Delta I = r_{SC-T} \left(\frac{G}{G_{ST}} \right) * (T_{ST} - T) + \left(\frac{G}{G_{ST}} - 1 \right) * I_{SC-ST} \quad (2)$$

$$\Delta V = -S_{OC-T} * (T_{ST} - T) - R_s * \Delta I \quad (3)$$

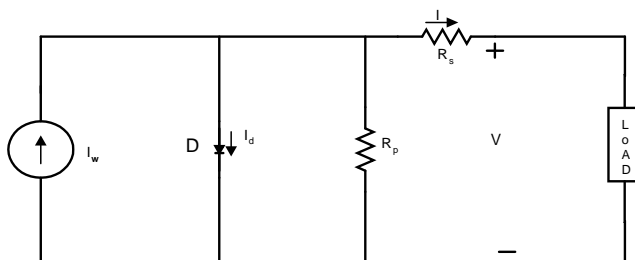


Fig.1.The equivalent Circuit of a Solar Cell.

Fig. 2 and Fig. 3 show I-V and P-V characteristics of 37 W_p solar panel, simulation is carried out using PSpice Software I_{sc} decreased significantly for varying solar radiation at constant temperature of 27°C.

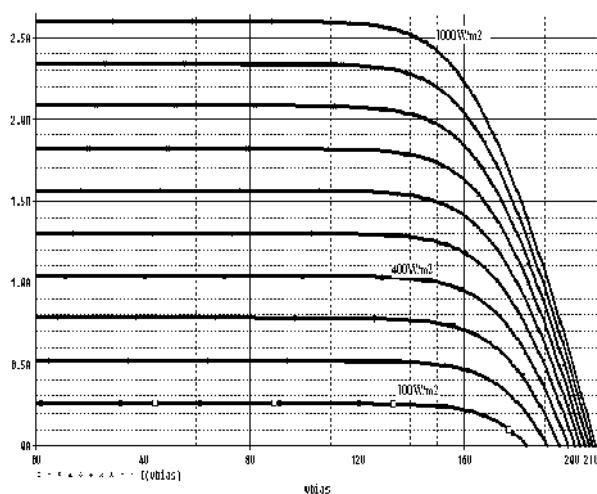


Fig.2. I-V characteristics of 37Wp solar panel panel of solar home lighting system

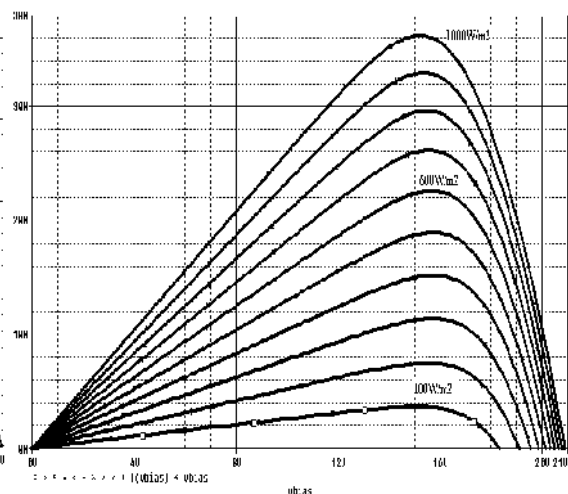


Fig. 3: P-V characteristics of 37Wp Solar solar home lighting System in VNIT

III. Soft Switching DC-DC Boost Converter

A) Design of Converter:-

The DC to DC boost converter has been designed using soft switching technique. The switching frequency is kept at an optimum value of 20KHZ for soft switching and PWM signal is generated

using Atmega32 microcontroller. MOSFETs IRFZ250 are used as main switch and auxiliary switch. Pot core is used to design filter inductance and main and resonant inductor.

Design equations 4 to 16 show behavior of Boost Converter and they are as follows

$$D = 1 - V_{in} / V_o \quad (4)$$

$$\Delta I = \frac{V_{IN}}{L} DT_s = \frac{V_o - V_{IN}}{L} (1 - D) T_s \quad (5)$$

$$\Delta I = 2 \times I_{IN} = \frac{V_{IN}}{L_{MIN}} DT_s \quad (6)$$

$$L_{MIN} = \frac{V_{IN}}{I_{IN}} \frac{D}{2f_s} = \frac{(1-D)DV_o}{\frac{1}{(1-D)}I_o f_s} = \frac{(1-D)^2 DR}{2f_s} \quad (7)$$

The soft-switching boost converter uses a simple auxiliary resonant circuit. It is composed of an auxiliary switch, a diode, a resonant inductor, and a resonant capacitor. During this interval, all switches in the adopted circuit perform zero-current switching by the resonant inductor at turn-on and zero-voltage switching by the resonant capacitor at turn-off. This switching pattern reduces the switching losses, voltage and current stress of the switching device. Fig.4 shows the circuit diagram of soft-switching of the DC-DC Boost converter used for the solar home lighting system. Switches S_1 and S_2 are MOSFETs IRFZ250. Capacitors C_1 and C_2 are Electrolytic Capacitors and Capacitor C_r is AC capacitor.

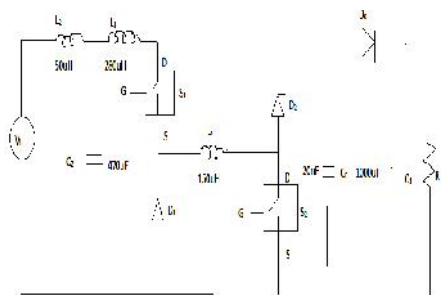


Fig.4 Circuit Diagram of Soft switching DC-DC boost converter

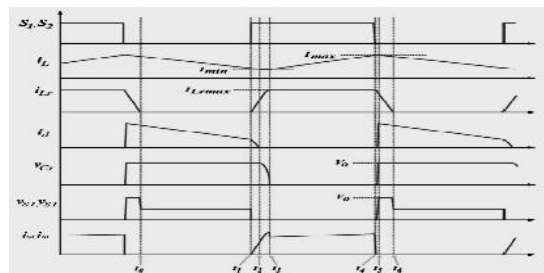


Fig.5: Theoretical Waveforms according to operational intervals

The adopted converter is controlled by ATmega32 microcontroller. The auxiliary circuit consists of an auxiliary switch (S_2), a resonant capacitor (C_r), a resonant inductor (L_r), and two diodes (D_1 and D_2). The converter operates in six intervals. For a simplification of analysis of each interval of this converter, the following assumptions are taken.

1) All used switching devices and passive elements are ideal. 2) There are negligible parasitic components of all switching devices and elements. 3) The input voltage (V_s) from solar Panel is in the range of 15 to 17.5V on load. 4) This converter is operated in continuous conduction mode at all intervals. Figure 5 shows the theoretical waveforms of the boost converter in various modes.

H.1. Interval 1 ($t_0 < t < t_1$)

In this mode, switches S_1 and S_2 are both OFF. The stored energy of the main inductor is transferred to the load with zero current in switches S_1 and S_2 . The modes are shown in Fig. 6. In this interval, the main inductor current decays linearly with nil current in resonant inductor. The resonant capacitor are charged up to output voltage.

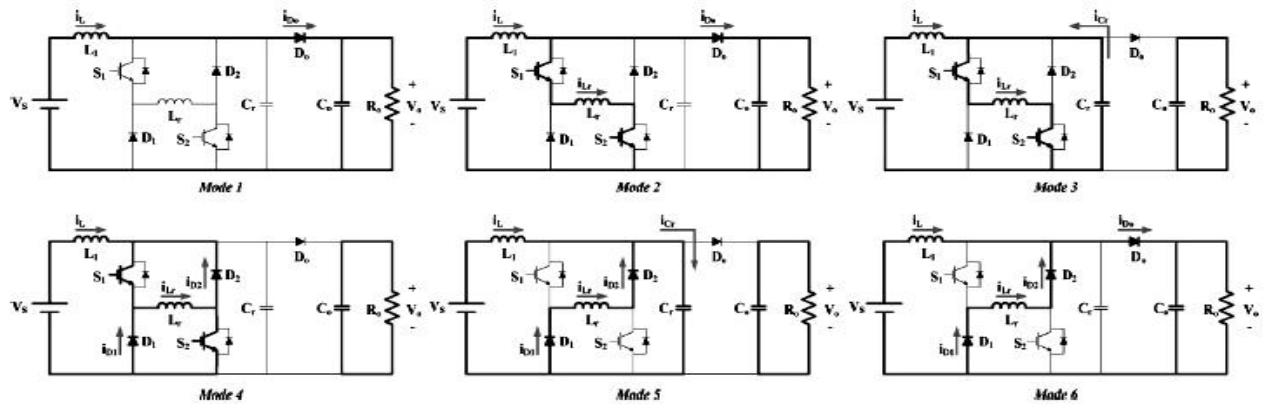


Fig. 6. Operational modes of the soft-switching boost converter for the PV generation system.

After turning on the two switches, interval 1 is over. These conditions are described as follows:

$$\begin{aligned} i_{D_o}(t) &= i_L(t) \\ V_L(t) &= V_s - V_o, i_L(t) = i_L(t_o) - \frac{V_o - V_s}{L}t, i_{L_r}(t) = 0 \\ v_{Cr}(t) &= V_o \end{aligned} \quad (8)$$

H.2 Interval 2 ($t_1 < t < t_2$)

Once switches S_1 and S_2 are turned on, the current flows through the resonant inductor. Since current is zero through two switches during switch turn on time, it is called as zero-current switching (ZCS) condition and thereby achieving low loss as compared to hard switching converter. Here the resonant current rises linearly, and the load current slowly decreases. At t_2 , current through the main inductor becomes equal to the resonant inductor current, and the output current of the diode is zero. When the voltage of the resonant capacitor equals V_o , the output diode becomes off, and finally the interval 2 is over

$$i_{L_r}(t_1) = 0, v_{L_r}(t) = V_o, i_{L_r}(t) = \frac{V_o}{L_r}(t), i_L(t) = i_L(t_1) - \frac{V_o - V_s}{L}(t), i_L(t_2) = i_{L_r}(t_2), i_{D_o}(t_2) = 0 \quad (9)$$

H.3 Interval 3 ($t_2 < t < t_3$)

The current which was flowing earlier to the load through output diode D_o no longer flows since t_2 . After this resonant capacitor C_r , and the resonant inductor L_r starts a resonance. The current flowing to the resonant inductor is addition of the main inductor current and the resonant capacitor current. The resonant current is expressed as

$$\begin{aligned} i_L(t) &= i_{\min}, i_{L_r}(t) = i_{\min} + \frac{V_o}{Z_r} \cdot \sin \tilde{S}_r, v_{Cr}(t) = V_o \cdot \cos \tilde{S}_r, v_{Cr}(t_2) = V_o, v_{Cr}(t_3) = 0 \\ \tilde{S}_r &= \frac{1}{\sqrt{L_r \cdot C_r}}, Z_r = \sqrt{\frac{L_r}{C_r}} \end{aligned} \quad (10)$$

This period is called as resonant period. During this period, the resonant capacitor C_r is discharged from V_o to zero. This is shown in (13). Resonant frequency and impedance is also shown. When the voltage of the resonant capacitor becomes zero, the interval 3 is over

H.4 Interval 4 ($t_3 < t < t_4$)

After completion of the resonant period in interval 3, the voltage of the resonant capacitor equals zero, and thus starts interval 4. In this interval, the freewheeling diodes D_1 and D_2 are turned on, and the current of the resonant inductor reaches maximum. The resonant inductor current flows to the freewheeling diodes in the sequence $S_1-L_r-D_2$ and $S_2-L_r-D_1$.

$$i_{L_r}(t) = i_L(t) + i_{D_1}(t) + i_{D_2}(t), i_{L_r}(t_3) = i_{L_r}(t_4) = i_{L_r \max}, V_L(t) = V_s, i_L(t) = i_{\min} + \frac{V_s}{L}t. \quad (11)$$

During this time, the main inductor voltage equals the input voltage. The current accumulating energy increases linearly.

H.5 Interval 5 ($t_4 < t < t_5$)

In interval 5, all switches are turned off under the zero voltage condition with the help of resonant capacitor. During this interval, the initial conditions of the resonant inductor current and resonant capacitor voltage are as shown in (15). After turning off all the switches, the resonant capacitor C_r is charged to the output voltage by two inductor currents. The output diode is in the OFF state until the resonant capacitor has been charged to V_o ,

$$\begin{aligned} i_{L_r}(t_4) &= i_{L_r \max}, V_{C_r}(t_4) = 0, i_L(t) = I_{\max}, i_{L_r}(t) = I_{\max} - (I_{\max} + I_{L_r \max}) \cdot \cos \tilde{S}_r t \\ v_{L_r}(t) &= Z_r \cdot (I_{\max} + I_{L_r \max}) \cdot \sin \tilde{S}_r t, v_{C_r}(t_5) = V_o \end{aligned} \quad (12)$$

H.6 Interval 6 ($t_5 < t < t_6$)

The last interval 6 begins once the resonant capacitor equals the output voltage. Later the output diode becomes on under the zero voltage condition (ZVS). During this interval, the main inductor current I_L resonant inductor current I_{L_r} flow towards the output through the output diode D_o

$$i_{D_o}(t) = i_L(t) + i_{L_r}(t), i_{L_r}(t_5) = (I_{\max} + I_{L_r \max}) \cdot \cos \tilde{S}_r(t_5 - t_4) - I_{\max}, v_{C_r}(t) = V_o \quad (13)$$

$$i_L(t) = I_{\max} - \frac{V_o - V_s}{L_r}t, i_{L_r}(t) = i_{L_r}(t_6) - \frac{V_o}{L_r}t, i_{L_r}(t_6) = 0 \quad (14)$$

Finally the energy of the resonant inductor is completely transferred to the load. Then, the interval 6 is finished. Values of resonant inductor (L_r) and resonant capacitor (C_r) are calculated by using below formulae 18 and 19.

$$L_r < \left(\frac{2}{\pi} D_{\min} * T * V_0 - V_{fw} * D_{\max} * T \right) / \left(\Delta i_L + \frac{2}{\pi} * I_{\min} \right) \quad (15)$$

$$C_r = \frac{0.04 D_{\min}^2 T^2}{\pi^2 * L_r} + \frac{4 I_{\min}^2 L_r}{\pi^2 V_o} - \frac{0.8 I_{\min} D_{\min} T}{\pi^2 V_o} \quad (16)$$

Where, V_{fd} = freewheeling voltage drop, Δi_L = current ripple of main inductor, I_{\min} = minimum current of main inductor, D_{\min} = minimum duty cycle, D_{\max} = maximum duty cycle, V_0 = output voltage. The output of the DC-DC Boost converter is verified by connecting 10/20 W DC lamp load and different current and voltage waveforms are taken.

Using various formulae mentioned above the Boost Converter has been designed.

B). Simulation Results

Using Multisim 10 software the DC to DC soft switching converter is simulated and output waveforms are observed. Figure 7 shows simulation diagram. The designed boost converter is simulated and various waveforms of the parameters like $V_{DS(S1)}$, $V_{DS(S2)}$, V_{Lr} , I_{Lr} , V_{Cr} , I_{S1} , V_{L1} and output boosted voltage V_o . Figures 8-17 show the simulated waveforms of soft switching DC-DC Boost converter.

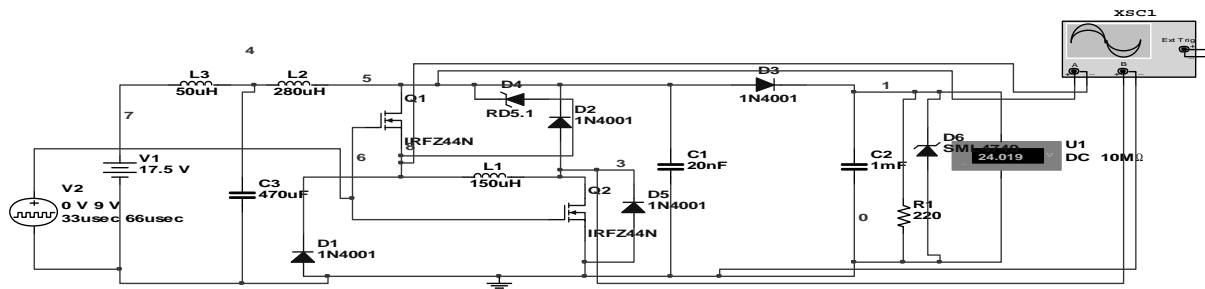


Fig.7 Simulation diagram of soft switching of DC-DC Boost converter

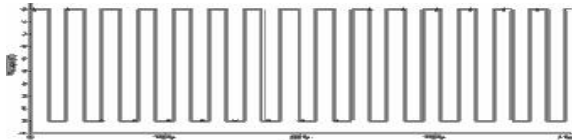


Fig.8. Gate pulses applied to main switch and resonant switch



Fig.9. Waveform of voltage across main switch

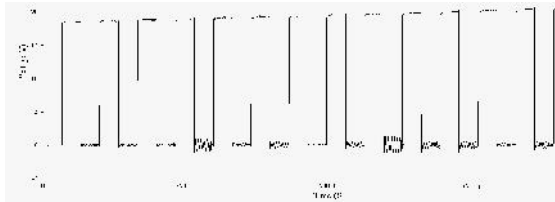


Fig.10. Waveform of Voltage across resonant switch

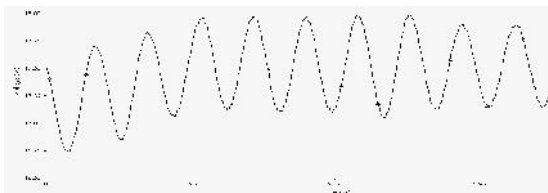


Fig.11. Voltage across input filter capacitor

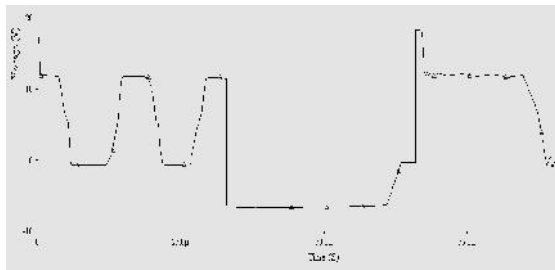


Fig.12. Voltage across resonant inductor

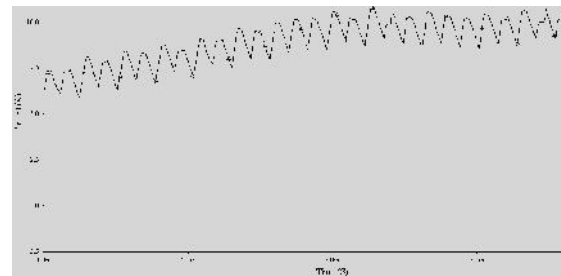


Fig.13 Waveform of Resonant Inductor Current

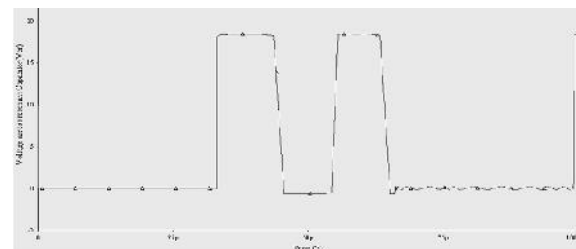


Fig.14. Waveform of Resonant Capacitor Voltage

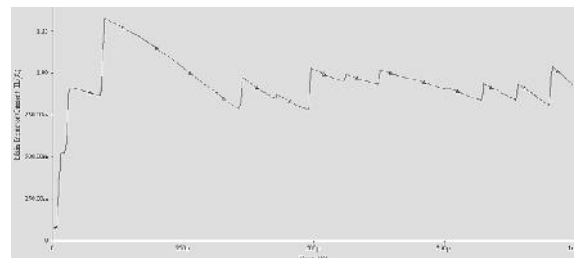


Fig.15: Waveform of Main Inductor Current

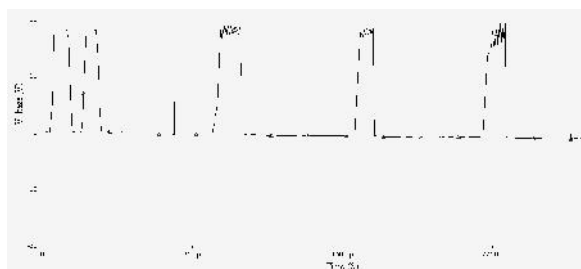


Fig.16.Voltage across main inductor

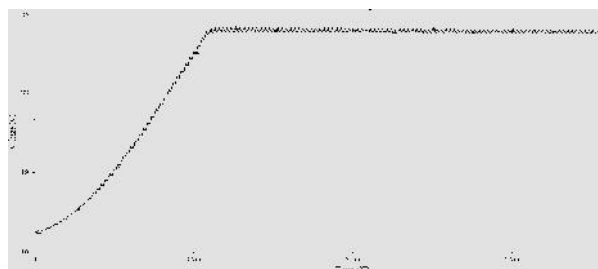


Fig.17.Output boosted DC voltage

C. Experimental Results of soft switching boost converter

The experimental results of the soft switching boost converter are generated using microcontroller Atmega32. Figure 18 shows PWM waveform generated at switching frequency of 15-20KHZ using Atmega32 Microcontroller. The waveforms are verified using Caddo make 9100 series DSO. For generating current waveforms, voltage waveforms have been taken across 1 resistor which is connected in series in the current carrying path.

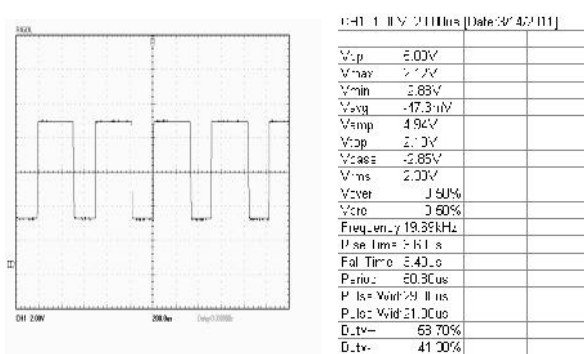


Fig.18. PWM waveforms of variable duty cycle through microcontroller Atmega32

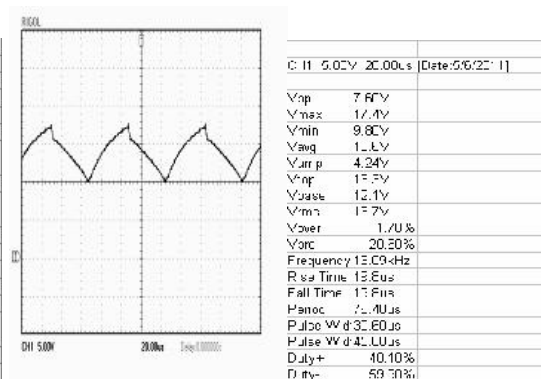


Fig.19.Waveform of input voltage of solar panel

Figures 20-24 show the experimental results of the boost converter.

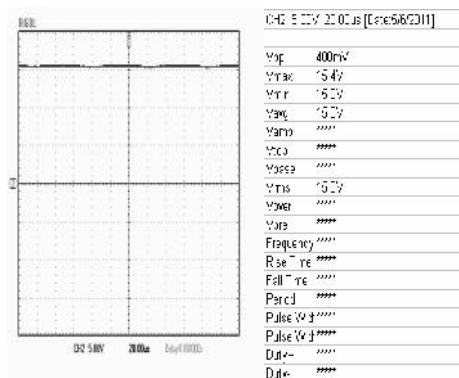


Fig.20.Waveform of input voltage after on LC filter from solar panel on 20W DC lamp load

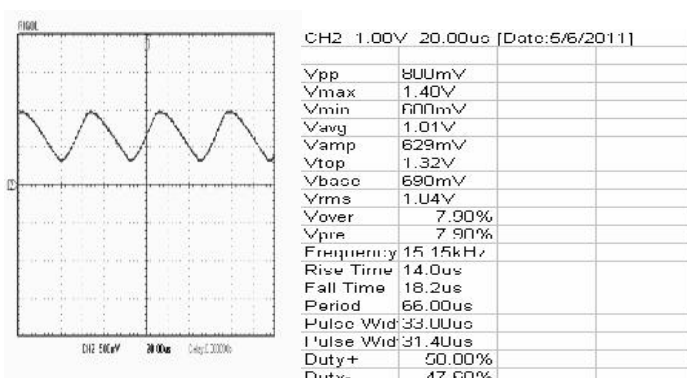


Fig.21 waveform of input current from solar panel 20W DC lamp load

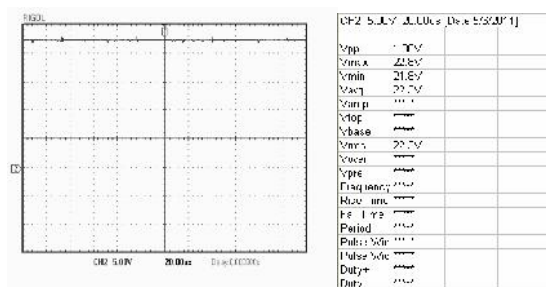


Fig.22 Waveform of load voltage on 20W DC lamp load

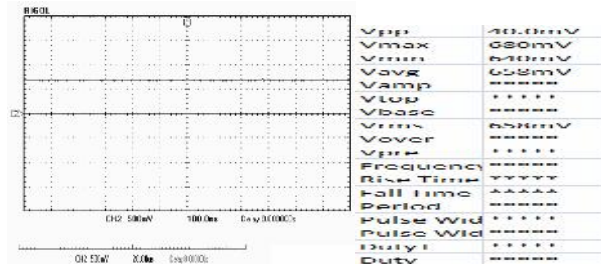


Fig.23 Waveform of load current on 20W DC lamp load

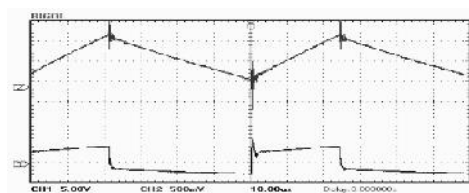


Fig.24 waveforms of inductor current with gate pulses

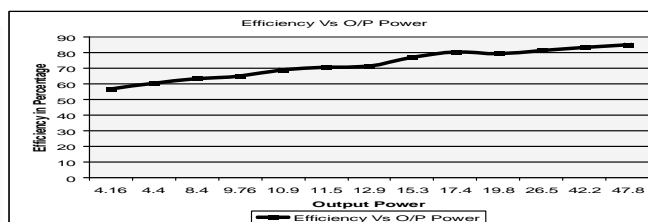


Fig.25. Efficiency as a function of output power

Figure 25 shows the Efficiency for soft switching Boost Converter as a function of output power with Rheostat. For increasing the load up to 48W, and analyze the efficiency curve for more load, one more panel of 75Wp was connected in parallel to 37Wp panel. The maximum efficiency is up to 87% for a load of 48W at a constant frequency of 15 KHz.

IV. Simulation Analysis of Maximum Power Point ZVS Boost Converter using Multisim 10.0

Fig. 26 shows the general block diagram of MPP scheme using constant voltage/current method. For simulation purpose, we used constant voltage method. Fig.27 shows the simulated implemented diagram of MPP using constant voltage method for soft switching boost converter. Table 1 shows the output readings generated through simulation.

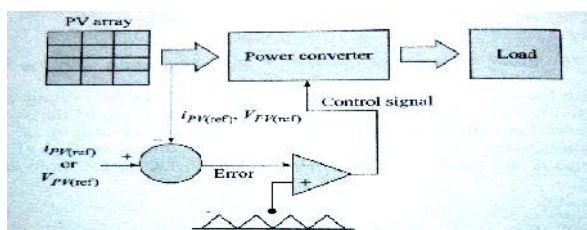


Fig. 26.MPPT Circuit for Constant Current/Constant Voltage Method

Table 1: - Simulated readings of V_{mpp} and I_{mpp}

Sr. No.	Maximum Power Point Voltage, V_{mpp} In Volts	Maximum Power Point Current, at the output side with boosted voltage of 24V
1	13.8	0.03
2	14.5	0.06
3	14.0	0.09
4	15.1	0.12
5	15.2	0.15
6	15.4	0.18
7	15.5	0.21
8	15.6	0.27
9	15.7	0.72
10	15.8	0.75
11	15.9	1.02
12	16.2	1.1

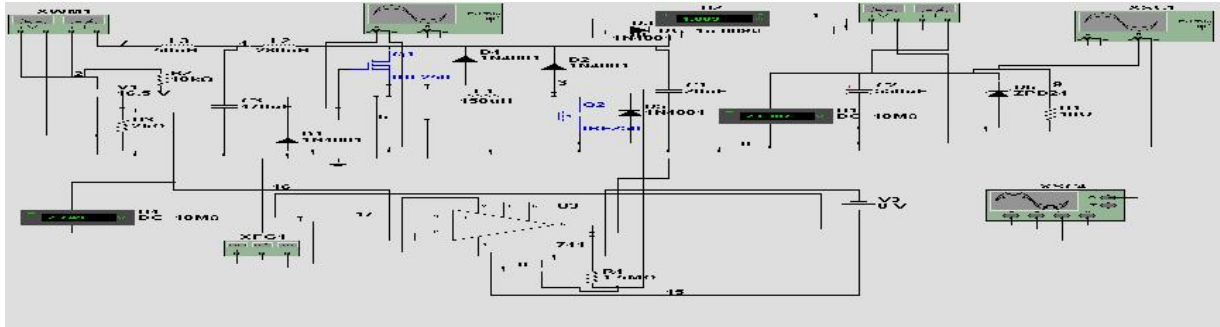


Fig.27:-Simulation diagram of Maximum Power Point Control of boost converter

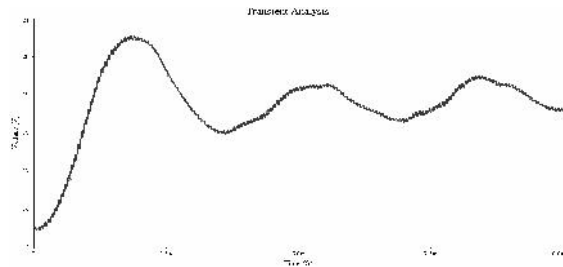


Fig. 28:- Maximum Power Point Voltage

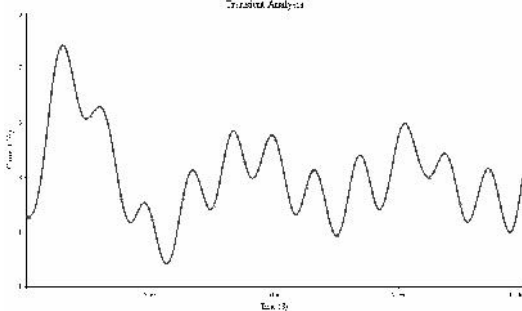


Fig. 29:- Maximum Power point Current

Figures 28 and 29 show the waveforms of Maximum power point voltage and current.

Table 2 shows the specification and Implementation Details of soft switching boost converter

Figures 30, 31 and 32 show the photographs of Atmega 32 microcontroller kit used for programming and Boost converter implementation respectively

Table 2: Boost Converter Specifications and Implementation Details

Maximum Power	$P_{o, \max}$	37+75(optional) =112W
Switching frequency	f_s	20 KHz
PV Module Voltage	V_i	15-17.5V
Output Voltage	V_o	27V
Main Inductor	L	280 μ H
Resonant Inductor	L_r	150 μ H
Input Filter Inductor	L_f	50 μ H
Output Capacitor	C_o	1000 μ F
Main Switch	S1	IRFZ250 Mosfet
Auxiliary Switch	S2	IRFZ250 Mosfet
Output Diode	D	24V Zener Diode (5W)
Microcontroller	Atmel	Atmega32



Fig.30 Atmega 16/32 programmer And development kit

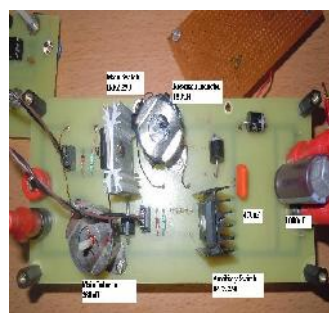


Fig.31 Photograph of Soft switching boost converter



Fig.32 Boost Converter with lamp load of 20W

V. Conclusion

The conclusions based on the present work are as under-

- Efficiency of Soft switching boost converter is in between 80 to 90 % for a load variation upto 47W
 - The Simulation of MPP is verified on Multisim software
- Future work is aimed to verify the simulation results of Maximum power point on hardware.

Appendix (Specifications of Solar Home Lighting System in EE Dept.)

Solar Photovoltaic Panel 12V, 37Wp Battery: - Low maintenance Exide 12V, 75 Ah, Solar PV Charge Controller: - -Max. Charging current - 5 A-Max. Load current - 5 A-Nominal voltage - 12 V - Fuse - 5A, DC Fan:-Volts – 12 V DC, 14 W, Compact Florescent Lamps Volts – 12 V DC, 9 W, Qty- 2 No.s

Acknowledgements

The authors are thankful to Visweswarayya National Institute of Technology and St. Vincent Pallotti College of Engg. And Technology, Nagpur, Maharashtra, INDIA for providing the facilities to carry out the research work in the laboratories.

References

1. Kolhe Mohan “Techno-Economic Optimum sizing of a stand-alone solar photovoltaic system”; IEEE transactions on energy conversion, Vol.4 No.2, June 2009, pp 511-519.
2. Masoum Mohamad A.S., Mahdi Seyed, Badejani Mousavi and Fuchs Ewald F.”Microprocessor Controlled new class of optimal battery chargers for photovoltaic applications”, IEEE transactions on energy conversion, Vol.19. No.3, September 2004, pp 599-606.
3. Boico Florent and Lehman Brad and Shujaee Khalil, “Solar Battery Chargers for NiMH Batteries” IEEE transactions on Power Electronics, Vol.22 No.5, September 2007, pp 1600-1609.
4. Moharil R. M. and Kulkarni P. S., “A case study of Solar Photovoltaic Power System at Sagardeep Island, India”, International Journal Renewable and Sustainable Energy Reviews (Elsevier Publication), Vol. 13, 2009, pp. 673-681.
5. Farahat, Metwally and Mohamed,” Optimal choice and design of different topologies of DC DC converter used in PV systems, at different climatic conditions in Egypt”, Elsevier Journal on Renewable Energy, Vol. 43, 2012, pp393-402.
6. Park Sang Hoon, Cha Gil-Ro, Jung Yong-Chae and Won Chung-Yuen, “Design and Application for PV Generation System Using a Soft-Switching Boost Converter with SARC”, IEEE Transaction On Industrial Electronics, vol.57, No.2, February 2010 pp-515-522.
7. Lee J.H., Bae H.S. and Cho B.H. “Resistive control for a photovoltaic Battery Charging System using a Microcontroller”, IEEE Transactions on Industrial Electronics, vol.55, No.7, July 2008, pp-2767-2775.
8. Long X., Liao R. and Zhoul J. “Low-cost charge collector of photovoltaic power conditioning system based dynamic DC/DC topology” IET Renew. Power Gener., 2011, Vol. 5, Iss. 2, pp. 167–174.
9. Tofighi A. , Kalantar M., “ Power management of PV/battery hybrid power source via passivity-based control” Elsevier Journal on Renewable Energy, Vol. 34, 2011, pp815-826.
10. Teng Tun-Ping , Nieh Hwa-Ming , Chen Jiann-Jyh , Lu Yu-Cheng, “ Research and development of maximum power transfer tracking system for solar cell unit by matching impedance”, Elsevier Journal on Renewable Energy, Vol. 35, 2010, pp845-851.
11. Masri Syafrudin, Chan Pui-Weng “Development of a Microcontroller-Based Boost Converter for Photovoltaic System” European Journal of Scientific Research, Vol.41 No.1 (2010), pp.38-47.

12. Werulkar A.S.,Kulkarni P.S., “Analysis of Microcontroller based Solar Charge Controller for Solar Home Lighting System”. International Conference on Advances in Energy Research (ICAER-2011), IIT, Bombay, India on December 9-11, 2011.
13. Werulkar A.S., Kulkarni P.S., “Design of a Constant Current Solar Charge Controller with Microcontroller based Soft Switching Buck Converter for Solar Home Lighting System”2012 IEEE International Conference on Power Electronics, Drives and Energy Systems(PEDES 2012),December 16-19,2012, Bangalore India.
14. Technical SESSION O-2.1.3, 978-1-4673-4508-8/12/\$31.00 ©2012 IEEE.
